The structure of the agrochemical fungicidal 4-chloro-3-(3,5-dichlorophenyl)-1*H*-pyrazole (RPA 406194) and related compounds

Jean-Pierre Vors,[a,*] Vincent Gerbaud,[b] Nadine Gabas,[b] Jean Paul Canselier,[b,*]
Nadine Jagerovic,[c] María Luisa Jimeno[c] and José Elguero[c,*]

[a]*Bayer CropScience, Centre de Recherche de La Dargoire, 14-20, Rue Pierre Baizet, B.P. 9163, F-69263 Lyon Cédex 09, France*
[b]*Laboratoire de Génie Chimique, ENSIACET, Institut National Polytechnique de Toulouse (INPT), BP 1301,*
*F-31106 Toulouse Cedex 01, France*
[c]*Instituto de Química Médica, C.S.I.C., Juan de la Cierva, 3, E-28006 Madrid, Spain*

Abstract—The difficulties to obtain convenient monocrystals of the important fungicide RPA 406194 have been overcome by a combination of solid state ^{13}C NMR, X-ray powder diffraction and molecular modeling. The compound, a 3-aryl tautomer, crystallizes forming infinite chains of molecules bonded by N–H⋯N hydrogen bonds, leading to needle-shaped crystals. The tautomerism (equilibrium constant and energy barrier) of this compound in solution has been studied. © 2003 Elsevier Science Ltd. All rights reserved.

1. Introduction

The search of new compounds for the protection of plants against fungal diseases led some of us to the discovery of a family of 1*H*-3(5)-arylpyrazoles bearing different substituents on the phenyl and the pyrazole rings.[1–4] Amongst the most active compounds are the derivatives **1**–**4** and particularly **1** (RPA 406194), represented below as 3-aryl derivatives, according to the rule that the most stable tautomer should be considered.[5–7] In this work we will discuss the structure of **1** and report some NMR data for the other three.
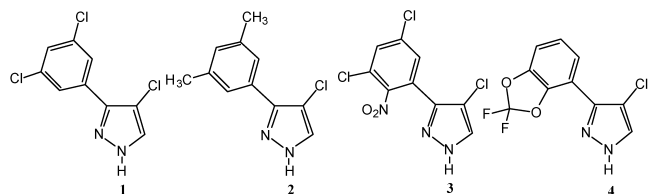

2. Results and discussion

Compounds **1**–**4** were described in Ref. 1 (the synthesis of **1** will be reported in Section 4). When we tried to obtain single crystals of **1** for X-ray diffraction, we encountered great difficulties. In general 1*H*-pyrazoles crystallize easily forming N–H⋯N hydrogen-bonded networks.[8] In some cases, the structure is difficult to solve (twins; several, up to 12, independent molecules in the unit cell, unstable polymorphs) but the crystals are always well shaped, transparent and of appropriate size. Compound **1** has a very strange behaviour which has consequences for its commercialization. Depending on the solvent used for its crystallization, the white powder has good (acetone), medium (acetonitrile) or bad (chloroform) properties. In the last case, the fluffy material forms a gel when mixed with water (suspension). However, the powder diffraction data of all samples are identical, excluding a problem of polymorphism.
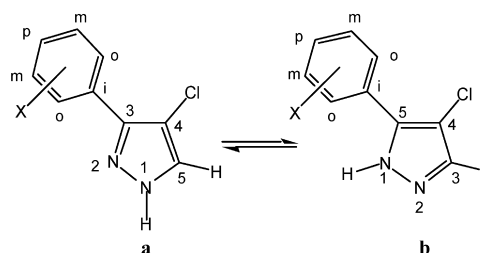
Scheme 1.

Table 1. ^{13}C chemical shifts of pyrazoles **1–4** (i, *ipso*; o, *ortho*; m, *meta*; p, *para*)

Compound	Solvent	C–aryl	C–Cl	C–H		Aryl group		
1[a]	CD$_3$OD	145.3	109.1	132.6		135.4 (i)	125.4 (o)	136.4 (m)
						128.9 (p)		
2	CDCl$_3$	142.1	107.8	135.3		128.8 (i)	125.0 (o)	138.3 (m)
						130.5 (p)	21.3 (Me)	
3	CDCl$_3$	146.5	108.6	129.4		127.3 (i)	126.8 (o H)	140.2 (o NO$_2$)
				136.0 (m H)		128.8 (m NO$_2$)	128.3 (p)	
4	CDCl$_3$	N.o.	109.2	133.5 (br)		113.4 (i)	122.3 (o H)	140.1 (o O)
						123.8 (m H)	143.9 (m O)	109.4 (p)
						131.3 (CF$_2$)		

[a] Broad signals; to observe those reported for C–aryl and C-5 a small amount of CF$_3$CO$_2$H has been added. N.o. not observed.

2.1. NMR study and the tautomerism of 3(5)-arylpyrazoles

Previous studies of the tautomerism of 3(5)-arylpyrazoles (including 4-halo derivatives) have shown that, in solution these compounds are mixtures of 3- (**a**) and 5-aryl tautomers (**b**) with predominance of tautomer **a**[9–13] (Scheme 1). In the solid state, several situations have been found: pure **a**, pure **b**, and 50:50 mixtures of **a** and **b**.[8,10,12,14]

The ^{13}C chemical shifts of pyrazoles **1–4** are gathered in Table 1.

For compounds **1**, **2** and **4** the spectra correspond to mixtures of both tautomers. The signal at 129.4 ppm (C–H) of compound **3** corresponds to tautomer **3a**.[9–13] Probably, the electron withdrawing character of the nitrodichlorophenyl substituent stabilizes **3a** with respect to **3b**. To determine the proportions of **a** and **b**, the ^{1}H spectrum of **1** was recorded at low temperature in CD$_3$OD.

The proton spectra of **1** in CD$_3$OD at various temperatures are reported in Table 2. At 21°C (294 K) the spectrum consists of two separate singlets. At 0 °C (273 K) it consists of three lines. Finally, the spectrum at 243 K showed six signals, three from the major tautomer (**1a**) and three from the minor tautomer (**1b**). Spectrum at 243 K was subjected to deconvolution in order to determine the population of the two tautomers (82.2% **1a** and 17.8% **1b**, K_T=4.6, average on three pairs of signals). Assignment was based on previous works.[9,10,14] These spectra were analyzed using the DNMR program (see Section 4). Barriers were estimated at 14.35 (294 K), 13.90 (273 K) and 13.2 kcal mol^{-1} (243 K), within the range of those determined for other pyrazoles.[7]

The lines corresponding to carbon atoms directly bonded to non-exchangeable protons were assigned from a ^{1}H–^{13}C g-HSQC spectrum (Table 3). This experiment was particularly useful since signals of the minor tautomer were hidden in the monodimensional spectra.

It is possible to use the ^{13}C NMR chemical shifts in methanol of Table 1 (average) and Table 3 (individual tautomers) to determine the equilibrium constant by interpolation. The best fit is obtained for almost exactly the same constant as that determined from ^{1}H NMR data (82.7% **1a** and 17.3% **1b**, K_T=4.8). This allows to predict that the missing values of the minor tautomer **1b** should be

under the signals of the major one at 148.2, 109.3 and 136.7 ppm.

Having determined the tautomeric structure in solution of compound **1** (82% **1a**–18% **1b**), as well as the predominance of **2a** over **2b**, the large excess of **3a** (>95% **3a**) and the predominance of **4a** over **4b**, we have studied these compounds by ^{13}C CPMAS NMR in the solid state (Table 4).

Some quaternary signals are not observed, e.g. the C–Cl one, split by scalar coupling with the quadrupolar chlorine atom linked to it.[16,17] The most important observation, based mainly on the ^{13}C–H chemical shifts, is that the four major tautomers (**1a**, **2a**, **3a** and **4a**) are 3-aryl derivatives. Therefore, in the solid state, C–aryl is C-3, C–Cl is C-4 and C–H is C-5.

2.2. X-Ray powder diffraction diagram of compound 1

The diagram corresponding to compound **1** is represented in Figure 1. We have not solved the structure using the Rietveld refinement procedure,[18] but we have instead used the following approach, based on the CERIUS2 package.[19] (i) Building of a starting structure for **1a**. (ii) Selection of a force field, Dreiding 2.21, which yields acceptable results in calculating crystal systems.[20] (iii) Optimization of molecular geometry. (iv) Minimization of the crystal lattice energy by means of CERIUS2. (v) Analysis of the final structure (crystal planes, hydrogen bonds, …). Out of the 230 space groups, we limited our search to the five most common in organic crystals (65% of all structures):[21] $P2_12_12_1$ (orthorhombic), $P2_1/c$ (or $P2_1/a$), $P2_1$, $C2/c$ (monoclinic) and $P\bar{1}$ (triclinic).

(i)–(iii) *Conformation of RPA 406194*. The minimization of the energy of RPA 406194 by means of the Dreiding 2.21 force field leads to the structure represented in Figure 2. There is a torsion angle of 33.3° between the phenyl and

Table 2. ^{1}H chemical shifts of tautomers **1a** and **1b** in CD$_3$OD

Compound	Temperature (K)	C–H	C-*ortho*	C-*para*
1a	294	7.82	7.82	7.46
1b	294	7.82	7.82	7.46
1a	273	7.89	7.83	7.48
1b	273	7.89	7.83	7.48
1a	243	7.95	7.84	7.51
1b	243	7.68	7.75	7.59

Table 3. [13]C chemical shifts of tautomers **1a** and **1b** in CD_3OD

Compound		C–aryl	C–Cl	C–H	Aryl carbon atoms			
					ipso	*ortho*	*meta*	*para*
1a	Experimental	148.2	109.3	131.0	136.7	126.8	136.7	129.3
	Predicted[a]	149.9	108.5	134.5	136.5	123.0	135.5	126.9
1b	Experimental	N.o.[b]	N.o.[b]	142.0[c]	130.1[c]	126.7[c]	N.o.[b]	129.5[c]
	Predicted[a]	141.3	108.5	139.5	131.9[c]	123.0[c]	135.5[c]	129.2

[a] Predictions based on 3(5)-phenylpyrazole[14] and chlorine effects on benzene.[15]
[b] N.o.—not observed.
[c] Determined from a ^{1}H–^{13}C g-HSQC spectrum.

pyrazole planes, which makes the compound chiral. This conformation corresponds to the isolated molecule in vacuo. We will assume that it will be maintained in the crystal.

(iv) *Structure of RPA 406194 in the crystal*. Using CERIUS2 we have calculated d_{hkl}, the spacing of the (*hkl*) set of planes, for structure **1** and compared them with the powder diagram (Fig. 1). The results are reported in Table 5 for the best solution.

Like biphenyl derivatives,[22] compound **1** presents axial chirality, thus existing in two conformations, *R* and *S* separated by a low energy barrier, that is, racemizing very quickly in solution. In our modelling work, we have assumed that the helix is formed exclusively by one enantiomer (*R* or *S*). It is evident that a crystal obtained from a racemic compound like **1** should contain the same number of *R* and *S* enantiomers. For a helix that means three possibilities: (i) helix formed by pairs of enantiomers $(R,S)_n$; (ii) a crystal containing both $(R)_n$ and $(S)_n$ helices; (iii) crystals formed by $(R)_n$ helices and crystals formed by $(S)_n$ helices (spontaneous resolution). In our review of the crystallization modes of NH-pyrazoles, there are two examples of non-planar phenylpyrazoles (compounds **19**, PAZDPY, and **31**, FAQSOF).[8] The first (torsion angle 4°) is an example of case (iii) while the second one (torsion angle ±46.7°) is an example of case (ii). Recently, we have determined the structure of 5-phenylpyrazole and it also belongs to case ii (torsion angle ±17.7°).[14] Since case (i) was never observed, we decided to assume that all the molecules in the chain have the same configuration.

The agreement between calculated and experimental d_{hkl} values is very good. In principle, it is possible to associate an experimental peak to each face. But, since some calculated d_{hkl} are very close: 5.7057, 5.7081 and 5.7811; 8.0382 and 8.0482, we have assigned them identical

experimental d_{hkl}: 5.7071 and 8.0021. These experimental values correspond to 5.5 and 7.76° angles. The atom coordinates in the unit cell are available from one of us (N. G.). In Figure 3 the location and orientation of the two independent, identical molecules of RPA 406194 in the unit cell are represented.

The structure of RPA 406194 corresponds to a chain (catemer) of N–H···N hydrogen bonded molecules. This is one of the motifs expected for 3-arylpyrazoles (the other is a cyclic trimer).[8]

In principle, it is possible to use molecular simulations to predict the morphology of crystals grown in vacuo if the space group and the crystal parameters are known. The method is based on the attachment energy, this magnitude being correlated to the growth rate of the different faces. Hartman's periodic bond chain (PBC)[23,24] theory (also called 'Hartman–Perdok-roughening-connected net')[25] classifies the crystal faces in three groups: F (flat) faces where the surface structure contains, strong intermolecular bonds (PBC) between atoms, ions or molecules of the crystal at least. In two non-parallel directions; S (stepped) faces corrugated, in one direction and with only one strong bond direction, and K (kinked) with no PBC, that are irregular with growth sites of vertex or edge types. The growth rates (in a perpendicular direction), V_i, for these faces are very different ($V_K \gg V_S \gg V_F$). To determine the morphological importance of these faces, the attachment energy E_{hkl} (negative) of the face (*hkl*) is calculated by molecular simulation from the crystal energy (E_{cr}) and the slice energy ($E_{sl(hkl)}$): $E_{hkl} = 1/2 (E_{cr} - E_{sl(hkl)})$.[24]

Moreover, when the crystal grows in spiral (BCF model),[26] that is, when the supersaturation is weak or moderate, V_{hkl} is an analytical function of E_{hkl}.[28,29] For a narrow range of attachment energies, the following relationship holds:[27] $V_{hkl} - |E_{hkl}|$. This relationship implies that the lower the

Table 4. [13]C chemical shifts of pyrazoles **1–4** (i, *ipso*; o, *ortho*; m, *meta*; p, *para*) in the solid state

Compd.	C–aryl	C–Cl	C–H	Aryl group			
1	146.1	105.8	132.6	136.9 (i)	125.0 (o)	136.0 (m)	130.1 (p)
		111.0					
2	N.o.	N.o.	135.8	128.2 (i)	125.3 (o)	137.7 (m)	128.2 (p)
				21.8 (Me)			
3	145.3	N.o.	129.7	N.o. (i)	128.0 (o H)	143.0 (o NO$_2$)	135.0 (m H)
				132.0 (m NO$_2$)	128.0 (p)		
4	N.o.	N.o.	133.5	113.6 (i)	122.4 (o H)	139.9 (o O)	115.0 (p)
					126.0 (m H)	142.9 (m O)	
				N.o. (CF$_2$)			

N.o.—not observed.

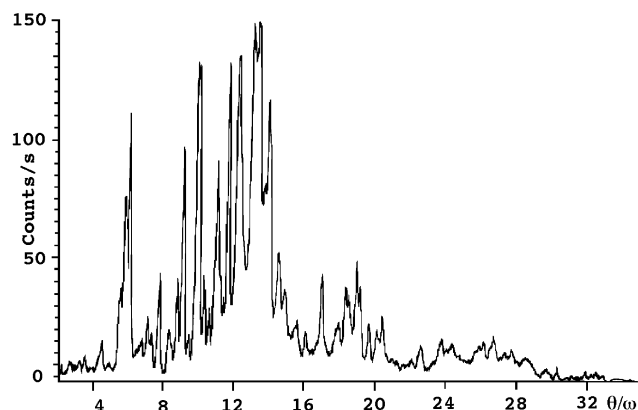**Figure 1.** Powder diffraction diagram of compound **1**.

Figure 3. Calculated crystal structure of compound **1**.

attachment energy of a (*hkl*) face in absolute value, the larger this face will be.

In Figure 4 the growth morphology in vacuo of a crystal of RPA 406194 is represented. Even if the solvent effect on morphology[30–35] has not been considered, the theoretical morphology has an elongated shape similar to the experimental morphologies (very fine needles in the best case, acetone). Probably this solvent, of moderate polarity, will increase the surface areas of the $\bar{1}00$, 001 and 101 faces, elongating the crystals.

3. Conclusion

The fungicide RPA 406194 corresponds, in the solid state, to the tautomer 3-(3,5-dichlorophenyl)-4-chloro-1*H*-pyrazole that crystallizes in the monoclinic $P2_1$ space group. The predicted elongated crystals are consistent with the fine needles observed.

4. Experimental

4.1. General procedures

Most NMR spectra in solution were recorded with a Bruker AC 250 instrument (Aventis). The solid state spectra were obtained from a Bruker MSL 400 spectrometer (CSIC). The ^{1}H and ^{13}C NMR spectra of compound 1 were taken on a
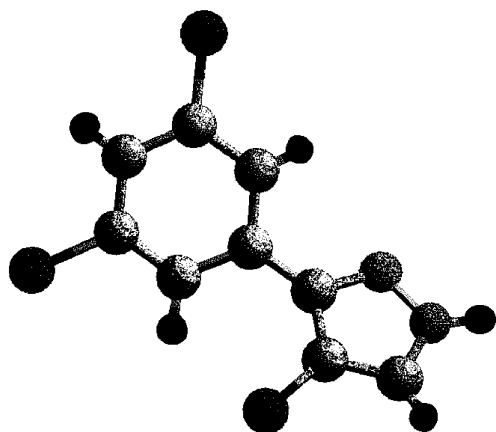
Varian Unity-500 spectrometer with a 5 mm inverse-detection H-X probe equipped with a gradient coil. The 1D spectra of **1** in CD_3OD were measured in the temperature interval 243–295 K with a digital frequency resolution of 0.1–0.2 Hz per point. The 2D g-HSQC spectrum was obtained using the standard Varian pulse sequence. The data were collected with 2048×128 data points, 8 scans for each increment. Spectral widths of 5000 and 30,000 Hz were used in the $F2$ (^{1}H) and $F1$ (^{13}C) domains, respectively. The calculation of the full shape of the ^{1}H NMR spectrum line was performed with the use of the gNMR v 4.0 program.[36] Activation parameters of the dynamic process were determined from the Eyring plot of the determined rate constants vs temperature (K). Calibration of the thermostat was performed by the registration of ^{1}H NMR spectra of methanol. A SEIFERT XRD 3000 TT diffractometer was used for the powder diffraction data collection.

4.1.1. 3-(3,5-Dichlorophenyl)-4-chloro-1*H*-pyrazole (1).
The condensation of 10 g (0.053 mol) of 3′,5′-dichloroacetophenone was carried out with 50 mL of DMF dimethyl-acetal during 2 h at 90 °C. After concentration of the reagent, 150 mL of heptane were added. 10.0 g of 1-(3,5-dichlorophenyl)-3-dimethylamino-2-propen-1-one were recovered after filtration (mp 100°C). 2.4 g (0.05 mol) of hydrazine hydrate were slowly added at room temperature to a solution of 9 g (0.0369 mol) of the enaminone in 100 mL of ethanol. After 2 h, the reaction mixture was
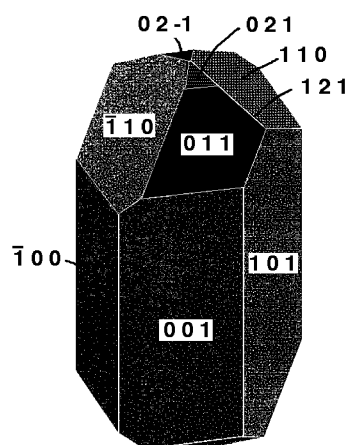

Figure 2. Minimum energy conformation of compound **1**.

Figure 4. Growth morphology of compound **1**.

Table 5. Comparison of the experimental and calculated d_{hkl} distances and intensities

d_{hkl} Exp	Intensity	d_{hkl} Exp	Intensity	h	k	l	d_{hkl} Calcd.	Closest d_{hkl} exp
9.8214	13.2	3.3583	148.7					
8.0021	38.3	3.2154	111.6					
7.6442	75.6	3.0833	48.3					
7.3093	109.2	3.0071	33.2	Visible faces in the morphology calculated from the theory of attachment energies				
6.5181	16.5	2.8722	20.9	0	0	0	8.0482	8.0021
6.2272	25.8	2.7878	15.8	1	0	1	8.0382	8.0021
6.0410	19.1	2.6437	40.0	1	0	1	5.7811	5.7071
5.7071	43.7	2.5069	19.9	1	−1	0	5.7081	5.7071
5.3292	19.2	2.4524	34.9	0	1	1	5.7057	5.7071
5.0574	38.3	2.4306	31.6	0	−1	1	5.7057	5.7071
4.8803	93.5	2.3780	45.8	1	2	1	3.3143	3.3583
4.7011	16.1	2.3521	35.0	1	−2	1	3.3143	3.3583
4.5088	128.5	2.2932	19.8	0	2	1	3.6142	3.6567
4.4483	127.7	2.2407	18.2	0	−2	1	3.6142	3.6567
4.3033	39.7	2.2090	23.0					
4.1948	26.1	2.0512	5.9	Other faces				
4.0371	87.5	2.0045	12.1	0	1	0	8.0900	8.0021
3.9050	30.0	1.9110	15.8	1	1	0	5.7021	5.7071
3.8237	128.3	1.8687	14.3	1	0	−1	5.5982	5.7071
3.6567	132.5	1.7496	15.2	1	1	1	4.7036	4.7011
3.4288	144.1	1.7145	18.2	1	1	−1	4.6035	4.7011

System: monoclinic; space group: $P2_1$; Z: 2; Cell parameters: a (Å)=8.04, α (°)=90, b (Å)=8.09, β (°)=76.99, c (Å)=8.05, γ (°)=90; density d_m (g cm^{-3})=1.61; lattice energy (kJ mol^{-1})=−126.

concentrated to dryness and the residue was triturated in hexane to give 7.1 g (mp 156°C) of 3-(3,5-dichlorophenyl)-1H-pyrazole. This pyrazole (2.3 g, 0.0152 mol) was chlorinated at room temperature in 300 mL of dichloromethane with 2.07 g (0.016 mol) of N-chlorosuccinimide during 4 days. The reaction mixture was then concentrated and the residue chromatographed on silica gel (heptane/ethyl acetate 70/30 v/v) to give 1.4 g of **1** (mp 192°C). Exact mass, calculated 247.95183, determined by mass spectrometry 247.95437. ^{1}H NMR (DMSO-d_6) 13.58, bs, NH; 8.07, s, C5-H; 7.81, d, J=1.8 Hz, 2H; 7.61, t, J=1.8 Hz, 1H.

References

1. Cantegril, R.; Croisat, D.; Desbordes, P.; Guigues, F.; Mortier, J.; Peignier, R.; Vors, J. P. PCT Int. Appl. WO 9322287 A1, November 11, 1993; *Chem. Abstr.* **1994**, *120*, 270382.
2. Cantegril, R.; Peignier, R. Fr. Demande FR 2705962 A1, December 9, 1994; *Chem. Abstr.* **1995**, *122*, 214067.
3. Cantegril, R.; Mortier, J.; Croisat, D.; Peignier, R. PCT Int. Appl. WO 9602138 A1, February 1, 1996; *Chem. Abstr.* **1996**, *124* 335658.
4. Chazalet, M.; Gouot, J. -M.; Peignier, R. PCT Int. Appl. WO 9843480 A1, October 8, 1998; *Chem. Abstr.* **1998**, *129*, 299238).
5. Elguero, J.; Marzin, C.; Katritzky, A. R.; Linda, P. *The Tautomerism of Heterocycles*; Academic: New York, 1976.
6. Elguero, J.; Katritzky, A. R.; Denisko, O. V. *Adv. Heterocycl. Chem.* **2000**, *76*, 1.
7. Minkin, V. I.; Garnovskii, A. D.; Elguero, J.; Katritzky, A. R.; Denisko, O. V. *Adv. Heterocycl. Chem.* **2000**, *76*, 157.
8. Foces-Foces, C.; Alkorta, I.; Elguero, J. *Acta Crystallogr. Sect. B* **2000**, *56*, 1018.
9. Cativiela, C.; García, J. I.; Elguero, J.; Elguero, E. *Gazz. Chim. Ital.* **1991**, *121*, 477.
10. Aguilar-Parrilla, F.; Cativiela, C.; Diaz de Villegas, M. D.; Elguero, J.; Foces-Foces, C.; Garcia, J. I.; Cano, F. H.; Limbach, H.-H.; Smith, J. A. S.; Toiron, C. *J. Chem. Soc., Perkin Trans. 2* **1992**, 1737.
11. Abboud, J. L. M.; Cabildo, P.; Cañada, T.; Catalán, J.; Claramunt, R. M.; De Paz, J. L. G.; Elguero, J.; Homan, H.; Notario, R.; Toiron, C.; Yranzo, G. I. *J. Org. Chem.* **1992**, *57*, 3938.
12. López, C.; Claramunt, R. M.; Trofimenko, S.; Elguero, J. *Can. J. Chem.* **1993**, *71*, 678.
13. Cativiela, C.; García, J. I.; Fayet, J.-P.; Elguero, J. *Bull. Soc. Chim. Belg.* **1995**, *104*, 383.
14. Pierrot, M.; Kenz, A.; García, M. A.; López, C.; Claramunt, R. M.; Elguero, J. In preparation.
15. Stothers, J. B. *Carbon-13 NMR Spectroscopy*; Academic: New York, 1972; p 197.
16. Olivieri, A. C.; Elguero, J.; Sobrados, I.; Cabildo, P.; Claramunt, R. M. *J. Phys. Chem.* **1994**, *98*, 5207.
17. Claramunt, R. M.; López, C.; García, M. A.; Otero, M. D.; Torres, M. R.; Pinilla, S.; Alarcón, S. H.; Alkorta, I.; Elguero, J. *New J. Chem.* **2001**, *25*, 1061.
18. Harris, K. D. M.; Tremayne, M.; Kariuki, B. M. *Angew. Chem. Int. Ed.* **2001**, *40*, 1627.

19. Accelrys Inc. (formerly, Molecular Simulations Inc., MSI).

20. Lommerse, J. P. M.; Motherwell, W. D. S.; Ammon, H. L.; Dunitz, J. D.; Gavezzotti, A.; Hofmann, D. W. M.; Leusen, F. J. J.; Mooij, W. T. M.; Price, S. L.; Schweizer, B.; Schmidt, M. U.; van Eijck, B. P.; Verwer, P.; Williams, D. E. *Acta Crystallogr. Sect. B* **2000**, *56*, 697.

21. Dunitz, J. D. *X-Ray Analysis and the Structure of Organic Molecules*; Cornell University Press: Ithaca, 1979.

22. Eliel, E. L.; Wilen, S. H. *Stereochemistry of Organic Compounds*; Wiley: New York, 1994; Chapter 12, p 1142.

23. Hartman, P.; Perdok, W. G. *Acta Crystallogr.* **1955**, *8*, 49.

24. Hartman, P. In *Crystal Growth: An Introduction*; Hartman, P., Ed.; North Holland: Amsterdam, 1973; p 367.

25. Bennema, P. In *Growth and Morphology of Crystals: Integration of Theories of Roughening and Hartman–Perdok Theory. Handbook of Crystal Growth*; Hurle, D. T. J., Ed.; North Holland: Amsterdam, 1993; Vol. 1, pp 477–581 Chapter 7.

26. Burton, W. K.; Cabrera, N.; Frank, F. C. *Trans. Roy. Soc.* **1951**, *A243*, 299.

27. Hartman, P. *J. Cryst. Growth* **1980**, *49*, 157. see also p 166.

28. Hartman, P.; Bennema, P. *J. Cryst. Growth* **1980**, *49*, 145.

29. Grimbergen, R. F. P.; Meekes, H.; Bennema, P.; Strom, C. S.; Vogels, L. J. P. *Acta Crystallogr. Sect. A* **1998**, *54A*, 491.

30. Berkovitch-Yellin, Z. *J. Am. Chem. Soc.* **1985**, *107*, 8239.

31. Weissbuch, Y.; Popovitz-Biro, R.; Lahav, M.; Leiserowitz, L. *Acta Crystallogr. Sect. B* **1995**, *51B*, 115.

32. Lin, C. H.; Gabas, N.; Canselier, J. P.; Pèpe, G. *J. Cryst. Growth* **1998**, *191*, 791.

33. Lin, C. H.; Gabas, N.; Canselier, J. P. *J. Cryst. Growth* **1998**, *191*, 803.

34. Winn, D.; Doherty, M. F. *AIChE J.* **1998**, *57*, 1805.

35. Winn, D.; Doherty, M. F. *Chem. Engng Sci.* **2002**, *44*, 2501.

36. *gNMR* v 4.0. Ivory Soft; Cherwell Scientific Publishing: Oxford, 1997.